GEOPHYSICAL RESEARCH LETTERS, VOL. 22, NO. 4, PAGES 365-368, FEBRUARY 15, 1995

Heating, ionization and upward discharges in the mesosphere due to intense quasi-electrostatic thundercloud fields

Victor P. Pasko[1], Umran S. Inan[1], Yuri N. Taranenko[2], and Timothy F. Bell[1]

Abstract. Quasi-electrostatic (QE) fields that temporarily exist at high altitudes following the sudden removal (e.g., by a lightning discharge) of thundercloud charge at low altitudes are found to significantly heat mesospheric electrons and produce ionization and light. The intensity, spatial extent, duration and spectra of optical emissions produced are consistent with the observed features of the Red Sprite type of upward discharges.

1. Introduction

Upward discharges are luminous glows occurring at altitudes ranging from cloud-tops to ~90 km [*Lyons*, 1994; *Sentman and Wescott*, 1993]. The Red Sprite type of upward discharges exhibit predominantly red color, enduring for few milliseconds and extending in altitude from ~50 to 90 km [*Sentman et al.*, 1994]. Ionospheric heating by electromagnetic pulses (EMPs) released in lightning [*Taranenko et al.*, 1993] produces ionization and light in a limited altitude range of 80-95 km. A new mechanism based on the heating of mesospheric electrons by QE thundercloud fields extends the altitude of the emitting region down to ~65 km and also accounts for the observed duration, spectra and spatial extent of the Red Sprites [*Sentman et al.*, 1994].

Following *Dejnakarintra and Park* [1974], we consider the electrical response of the upper atmosphere to large quasi-static charge distributions. We account for the nonlinear self-consistent dependence of the conductivity σ on the ionization and electron heating at different altitudes, and estimate the distribution of the resulting optical emissions.

2. Model Formulation

Red Sprites are typically associated with 1 out of 20-40 especially energetic positive cloud-to-ground (CG) discharges [*Sentman and Wescott*, 1993; *Sentman et al.*, 1994]. Positive CG discharges can involve transfer (to the ground) of up to 300 C in several ms [e.g., *Brook et al.*, 1982], resulting in large (up to ~1000 V/m at 50 km altitude) QE fields due to the uncompensated negative charge left in and above the cloud. The ambient electrons and ions at all altitudes above the cloud are heated by the large QE fields, leading to optical emissions. The observed several to tens of ms duration of Red Sprites is consistent with the characteristic relaxation time of QE fields due to finite conductivity of the medium [*Dejnakarintra and Park*, 1974; *Baginski et al.*, 1988].

We consider a QE field established in the mesosphere and lower ionosphere due to the accumulation of large thundercloud charge and its evolution in time when the charge is brought to the ground (exponentially with a time constant of 1 ms) by a CG lightning stroke. We use a cylindrical coordinate system (r, ϕ, z) with the z axis representing altitude. The ground and the cylindrical boundaries at z=90 km and r=60 km are assumed to be perfectly conducting. The effect of the artificial conducting boundary at r=60 km on the QE fields inside the system is small (e.g., ~10 % at r=50 km, z=10 km). The ambient ion conductivity is assumed to vary exponentially with altitude, with a scale height of 6 km [*Dejnakarintra and Park*, 1974]. The electron component of the ambient σ is based on the 'tenuous' ambient density model of *Taranenko et al.* [1993*a*], ionization rates for atmospheric and ionospheric breakdown of *Papadopoulos et al.* [1993], and the electron mobility as a function of electric field obtained from experimental data [*Davies*, 1983]. Electrons are assumed to have a small but non-negligible number density at mesospheric altitudes [*Reagan et al.*, 1981]. We neglect chemical effects due to their relatively long time scales [e.g., *Mitra*, 1981] and the geomagnetic field since the plasma is highly collision dominated even after minor heating.

We consider two different cases of charge accumulation and removal (Figure 1a); a monopole charge +Q or separated dipole charges +Q, -Q assumed to form in a thundercloud over a time τ_f (few seconds). The monopole or the positive half of the dipole charge is then discharged to ground with a time constant τ_s. In each case, as the charges accumulate, high altitude regions where τ_f is greater than the local relaxation time are shielded from the QE fields of the thundercloud charges by induced space charge at lower altitudes. When charge is quickly removed, a QE field appears at all altitudes above the shielding space charge. As we show below in section 3.2, this field is essentially identical for the monopole or dipole cases at altitudes >55 km. Since charge removal can be viewed as 'placement' of an identical charge of opposite sign, the initial field at ionospheric altitudes is approximately the free space field due to the 'newly placed' charge. Thus, the important physical consequences of the QE system depend on the magnitude and altitude of the removed charge and are essentially independent of the initial charge configuration. For simplicity, we first consider the monopole and discuss the dipole case in section 3.2.

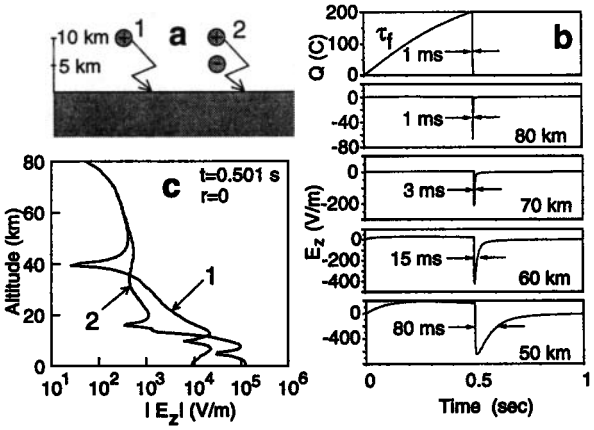

Figure 1. (a) Monopole (1) and dipole (2) models of thundercloud charge; (b) The assumed behavior of the source charge (top panel) and the corresponding establishment and relaxation of E_z at selected altitudes at r=0 km; (c) Altitude distribution of $|E_z|$ at t =0.501 s for two cases shown in (a).

[1] STAR Laboratory, Stanford University, Stanford, CA

[2] NIS-1, MS-D466, Los Alamos National Laboratory, Los Alamos, NM

Paper number 95GL00008
0094-8534/95/94GL-00008$03.00

The space-time variation of the QE field $\vec{E} = -\nabla\varphi$ (where φ is the electrostatic potential) and charge density ρ are governed by the following system of equations:

$$\frac{\partial \rho}{\partial t} - \nabla \cdot [\sigma \nabla \varphi] = 0 \quad (1)$$

$$\nabla^2 \varphi = -(\rho + \rho_s)/\varepsilon_o \quad (2)$$

where $\rho_s(\vec{r}, t)$ is the source charge density which is assumed to have a Gaussian spatial distribution ($e^{-[(z-z_o)^2+r^2]/a^2}$) with z_o=10 km, a=3 km so that the total source charge $Q(t) = \int \rho_s(\vec{r}, t)dV$. Below we represent $Q(t)$ by its maximum value (100, 200 or 300 C), the charge separation time (τ_f=0.5 s) and the time of charge removal (i.e., duration of the CG discharge) taken to be an exponential with decay τ_s=1 ms.

We integrate equations (1), (2) numerically following *Potter* [1973, p.34] and *Swarztrauber and Sweet* [1975]. In (1) σ is calculated self-consistently by taking into account the effect of the QE field on the electron component through changes in mobility (due to heating) and number density (due to ionization). The optical emissions are calculated using known functions and crossections for impact excitation of electron levels of ambient N_2 [*Taranenko et al.*, 1993].

3. Results

3.1. Electric Field and Charge Density. Figures 1b and 2 show results for Q=200 C. The slow (0.5 s) build-up of $Q(t)$ leads to the formation of small but finite steady state QE fields (Figure 1b) which are similar in nature to the fair weather electric field produced by charges maintained on Earth [e.g., *Uman*, 1974]. The removal of charge with a time constant τ_s=1 ms leads to (Figure 1b) QE fields of up to ~100 V/m, lasting for several ms at ionospheric altitudes.

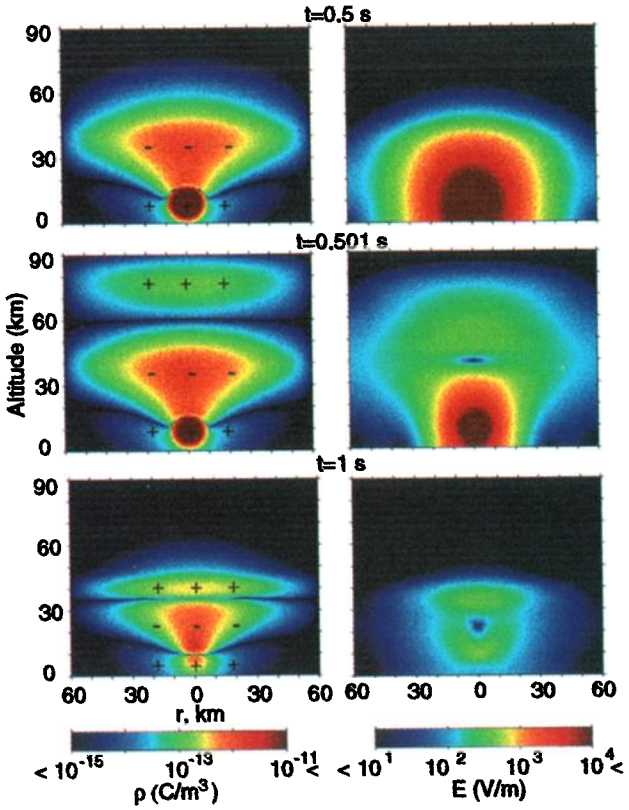

Figure 2. A sectional view of the distribution of the absolute values of ρ (left panels) and $\vec{E}$ (right panels) at selected instants of time. At t=0.501 s the source charge (middle left panel) has decreased by a factor of e^{-1} but appears roughly at the same level as that in the top left panel due to the limited dynamic range of the color display.

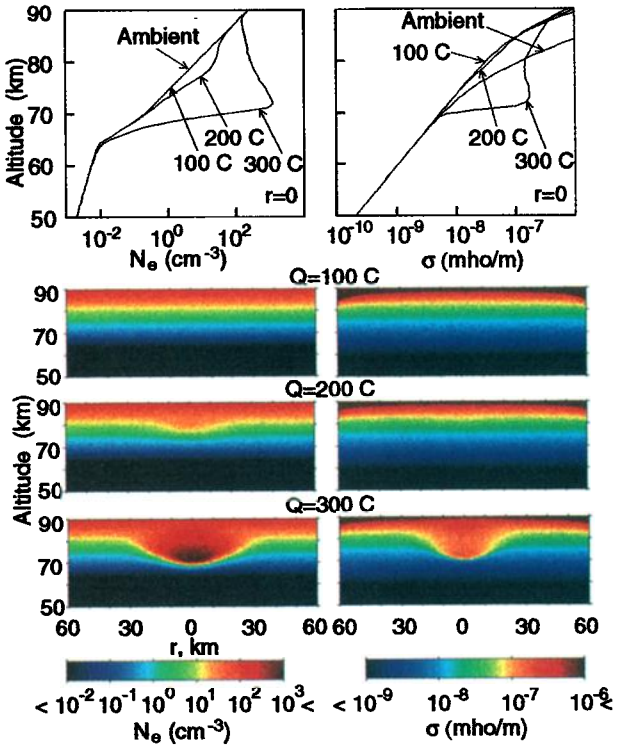

Figure 3. The altitude distribution of the N_e (left) and σ (right) for different Q at t =0.501 s. The top panels show altitude scans at r=0.

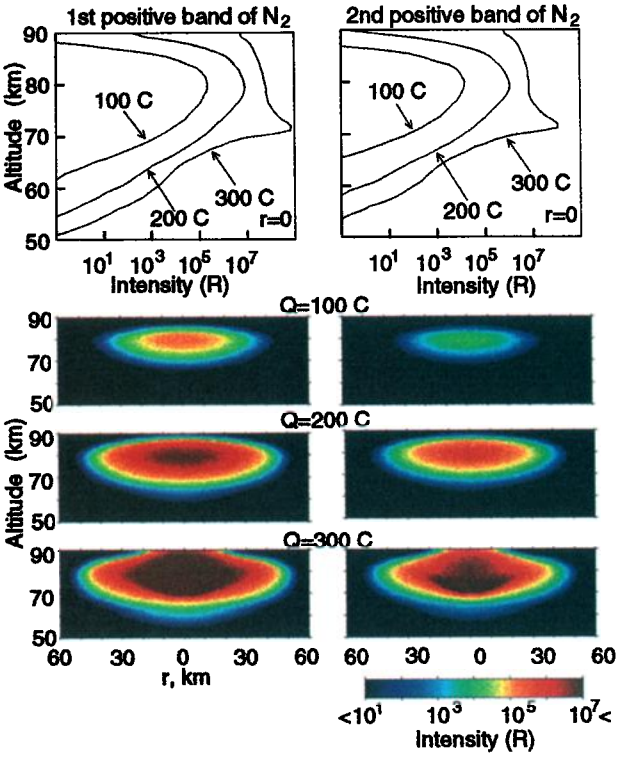

Figure 4. The distribution of intensities (Rayleighs) of emissions of the 1st (left panels) and 2nd (right panels) positive bands of N_2 at t =0.501 s for different source charge values. Two top panels show the corresponding quantities as functions of altitude at r=0.

Figure 2 shows the spatial distribution of ρ and $\vec{E}$ just before (t =0.5 s) and 1 ms after the initiation (t =0.501 s) of the CG lightning and at the end of the simulation (t =1 s). The 'explosive' appearance of $\vec{E}$ at higher altitudes at t = 0.501 s can be physically understood as follows: At steady state, free charges in the mesosphere and lower ionosphere redistribute (Figure 2, left panels) to create an $\vec{E}$ approximately equal and opposite to the 'applied' static $\vec{E}$ due to the large thundercloud charge. Once the thundercloud charge is removed, only the $\vec{E}$ due to the space charge remains, and this large field endures for a time determined approximately (see discussion below) by the local relaxation time ($\tau_r = \varepsilon_o/\sigma$) at each altitude.

3.2. Conductivity. Figure 3 shows the distributions of electron number density N_e and σ for Q=100, 200 and 300 C at t=0.501 s. The system exhibits a threshold dependence on Q; N_e does not change significantly for Q=100 C, whereas Q=200 and 300 C leads to changes in N_e by factors of ~4 (at 79 km) and ~10^4 (at 72 km) respectively. The changes in N_e result in corresponding changes in σ, although the net σ changes are determined by the interplay between changes in N_e (due to ionization) and electron mobility (due to heating). For example, the factor of ~10 decrease in σ at ~80 km altitude for Q=100 C and 200 C is dominantly due to electron heating, since N_e changes are relatively small. Maximum values of the mean energy of the electron distribution (obtained in the optical emission calculations (see section 3.3 below)) for Q=100 C, 200 C, and 300 C are 2.0, 4.4, and 5.1 eV, occurring respectively at altitudes of 79, 77 and 71 km.

The results in Figures 2 and 3 indicate that QE fields can reach substantial values, significantly changing N_e and σ at ~65 to 90 km altitudes in regions with ~50-60 km transverse extent. One manifestation of such σ changes in experimental data may be the so-called 'early' VLF signal perturbations observed in association with lightning discharges [*Inan et al.*, 1993]. Also, these σ changes modify the relaxation characteristics of $\vec{E}$ at ionospheric altitudes as discussed below.

For a dipole thundercloud charge configuration (Figure 1a), the $\vec{E}$ field as well as the N_e and σ changes at > 55 km altitudes are identical to those in Figures 2 and 3. Figure 1c shows a comparison of the QE field values which appear after the removal of positive thundercloud charge for both monopole and dipole cases. Since the QE fields for the two cases are essentially identical at z > 55 km, the heating, ionization and optical emission (dependent only on $|\vec{E}|$) results given below pertain to both the monopole and dipole cases.

3.3. Optical Emissions. The spatial distributions of optical emissions calculated for Q=100 C, 200 C and 300 C at t=0.501 s) are shown in Figure 4. The local optical emissivities of the first (red) and second (blue) positive bands of N_2 excited via impact excitation at different points in a cylindrically symmetric volume were integrated along horizontal lines to determine the emission intensities (I) in Rayleighs observed when viewed horizontally from a distant point. In all cases shown, I corresponding to the red band is ~10 times larger than that of the blue band, consistent with the dominant red color of the Red Sprites. For Q=300 C, I is larger than the typical reported intensity (~10-500 kR) of Red Sprites by more than a factor ~10^3 when viewed through the center of the heated region (at ~72 km). For Q=100 C and 200 C the maximum values are 250 kR and 9×10^3 kR (at ~81 km and ~79 km, respectively). Additional calculations for Q=30 C, 50 C and 75 C (not shown) give values of the maximum intensity of the first positive band of 15 R, 1 kR and 23.4 kR, respectively, demonstrating a highly nonlinear dependence on Q, consistent with the fact that the Red Sprites are associated with only the most intense lightning discharges.

The temporal duration of the observed luminosity at > 65 km altitudes is determined by the duration of the QE field, which relaxes with a time constant of ~1 ms at 80 km and ~3 ms at 70 km altitudes (see Figure 1b), consistent with the observed few ms duration of Red Sprites. The transverse extent of the region of most intense emission (the central red cores in Figure 4) is of order ~20-50 km, also consistent with the observed ~10-50 km horizontal extent of Red Sprites.

Quantitative experimental data on the altitude extent of Red Sprites is not yet published; however, our results are consistent with what is known at this time. The Red Sprites are well detached from the cloud-tops and typically extend to ~90 km, with maximum intensities at >80 km altitudes, at which our results exhibit broad maxima (Figure 4).

4. Discussion

4.1. Lightning Current and Charge. The density and conductivity changes as well as the light output have a threshold type of dependence on Q. The transfer of 100, 200 and 300 C with an exponential time constant of 1 ms corresponds to peak currents of 100, 200 and 300 kA, respectively, which are at the higher end of those observed for positive CG lightning [*Uman*, 1987, p. 123]. Parameter values used in our work are in general agreement with the impulsive transfer of 150 C with a stroke duration of 2 ms which may occur in ~5 % of lightning [*Uman*, 1987, p. 124]. However, positive flashes are generally composed of a single stroke followed by a period of continuing current [*Uman*, 1987, p. 20], so that the actual time of charge transfer could be longer. The results of our model are valid as long as the time of charge transfer does not significantly exceed the local relaxation time τ_r at 50-90 km altitudes. We note that ion conductivities lower than those used in our work (by factors of ~10^2 at 70 km) have been observed above thunderstorm regions [*Holzworth et al.*, 1985]. In such cases, τ_r would be longer, so that our results would be consistent with a wider range of times of charge transfer (τ_s). For example if τ_r=5 ms, the peak currents required would be only 20-60 kA. The peak emission intensities would not depend significantly on the ambient σ profile since the self consistent σ is determined largely by the magnitude of the QE field. The existence of separated charges of ~100 C at 10 km altitude is also consistent with aircraft-based measurements of *Blakeslee et al.* [1989], who reported intensities of up to 7 kV/m at ~20 km altitude.

The charge separation time ($\tau_f \simeq 0.5$) s used in our model is less than the typical times of tens of seconds between successive lightning discharges as observed [*Blakeslee et al.*, 1989] and as used in previous theoretical work [e.g., *Dejnakarintra and Park*, 1976]. However, the physics studied and the results are unchanged since $\tau_f \simeq 0.5$ s $\gg \tau_r$ at all altitudes of interest.

4.2. Relaxation Times of QE Fields. An important aspect of our model with respect to previous work on the relaxation of QE fields [*Dejnakarintra and Park*, 1974; *Baginski et al.*, 1988] is the self-consistent modeling of the conductivity σ. In Figure 5, we compare the temporal variation of $|E_z|$ at 70 and 80 km for three different models of σ. At z =80 km $|E_z|$

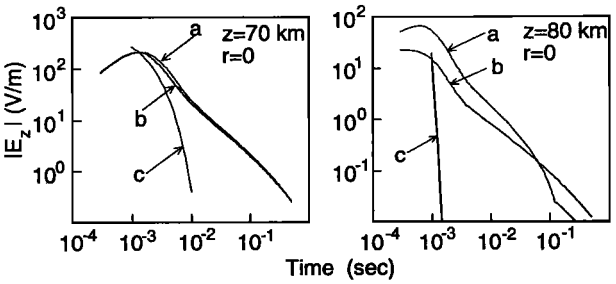

Figure 5. The vertical component $|E_z|$ at z=70, 80 km at r=0 as a function of time after the initiation of the lightning stroke for Q=200 C for different models of σ: (a) self-consistent model (this paper); (b) σ kept constant in time; (c) relaxation with the local ambient ε_o/σ.

for case (a) is ~4 times that for (b), and initially exhibits ~3 times longer time duration, followed by a faster decrease, resulting from the decrease of σ due to heating initially followed by its increase due to ionization at later times. The QE field at a given point depends on the charge distribution at surrounding points and does not relax with the local ambient rate (c) because in a medium with $\nabla\sigma \neq 0$ a local source current due to the 'external' electric field essentially introduces new local charge. In our particular system, charges relax much more slowly at lower altitudes (Figure 3), constituting a source of QE field at higher altitudes.

4.3. Comparison with EMP-induced heating. Taranenko et al. [1993] used a one dimensional fully kinetic and self consistent model to estimate optical emissions produced by the heating of the ambient electrons by lightning EMP at ~80-95 km altitudes. In this work, results were given for peak EMP intensities E_{100} (normalized to 100-km horizontal distance) of $E_{100} \leq 25$ V/m. In terms of our work, E_{100}=25 V/m corresponds to $Q \simeq 100$ C [*Orville*, 1991]. Results of *Taranenko et al.* [1993] indicate that optical emissions due to EMP-heating endure for shorter periods (~100μs) and exhibit a broad maximum at altitudes of ~90 km, higher that those excited by QE fields (Figure 4). Although comparisons of peak emission intensities are difficult since the transverse size of the EMP-heating is not known, estimates indicate that EMP-heating leads to brighter emissions at >80 km.

5. Summary

Our model of the Red Sprites is based on the local heating of mesospheric/lower-ionospheric electrons by intense QE fields resulting from large uncompensated charge distributions that temporarily exist in and above thunderstorms following removal of charge by lightning discharges. Results of self consistent two dimensional solutions are consistent with the observed spectra, temporal duration, and spatial extent of Red Sprites.

Acknowledgments. This work was sponsored by the NASA grant NAGW-2871 to Stanford University. The participation of Y. Taranenko was supported by a Los Alamos National Laboratory Post Doctoral Fellowship.

References

Baginski, M. E., L. C. Hale, and J. J. Olivero, Lightning-related fields in the ionosphere, *Geophys. Res. Lett., 15*, 764, 1988.

Blakeslee, R.J., H.J. Christian and B. Vonnegut, Electrical Measurements Over Thunderstorms, *J. Geophys. Res., 94*, 13135, 1989.

Brook, M., M. Nakano, P. Krehbiel, and T. Takeuti, The electrical structure of the Hokuriku winter thunderstorms, *J. Geophys. Res., 87*, 1207, 1982.

Davies, D.K., Measurements of swarm parameters in dry air, *Theoretical Notes*, Note 346, Westinghouse R&D Center, Pittsburg, May, 1983.

Dejnakarintra, M., and C. G. Park, Lightning-induced electric fields in the ionosphere, *J. Geophys. Res., 79*, 1903, 1974.

Holzworth, R. H., M. C. Kelley, C. L. Siefring, L. C. Hale and J. T. Mitchell, Electrical measurements in the atmosphere and the ionosphere over an active thunderstorm. 2. Direct current electric fields and conductivity, *J. Geophys. Res., 90*, 9824, 1985.

Inan, U. S., J. V. Rodriguez, and V. P. Idone, VLF signatures of lightning-induced heating and ionization of the nighttime D-region, *Geophys. Res. Lett., 20*, 2355, 1993.

Lyons, W. A., Characteristics of luminous structures in the stratosphere above thunderstorms as imaged by low-light video, *Geophys. Res. Lett., 21*, 875, 1994.

Mitra, A. P., Chemistry of middle atmospheric ionization - A review, *J. Atmos. Terr. Phys., 43*, 737, 1981.

Orville, R. E., Calibration of a magnetic direction finding network using measured triggered lightning return stroke peak currents, *J. Geophys. Res., 96*, 17135, 1991.

Papadopoulos, K., G. Milikh, A. Gurevich, A. Drobot, and R. Shanny, Ionization rates for atmospheric and ionospheric breakdown, *J. Geophys. Res., 98*, 17593, 1993.

Potter, D., *Computational physics*, John Wiley & Sons, London, 1973.

Reagan, J. B., R. E. Meyerott, R. C. Gunton, W. L. Imhof, E. E. Gaines and T. R. Larsen, Modeling of the ambient and disturbed ionospheric media pertinent to ELF/VLF propagation, in *Proceedings of NATO-AGARD Meeting on Medium, Long, and Very Long Wave Propagation*, Brussels, Belgium, 1981.

Sentman, D. D., and E. M. Wescott, Observations of upper atmospheric optical flashes recorded from an aircraft, *Geophys. Res. Lett., 20*, 2857, 1993.

Sentman, D. D., E. M. Wescott, D. L. Osborne, D. L. Hampton, M. J. Heavner, Preliminary results from the Sprites94 campaign: Red Sprites, *Geophys. Res. Lett.*, in review, 1995.

Swarztrauber, P., and R. Sweet, Efficient FORTRAN subprograms for the solution of elliptic partial differential equations, *NCAR Technical Note*, NCAR/TN-109+IA, July, 1975.

Taranenko, Y. N., U. S. Inan, and T. F. Bell, The interaction with the lower ionosphere of electromagnetic pulses from lightning: excitation of optical emissions, *Geophys. Res. Lett., 20*, 2675, 1993.

Uman, M.A., *The lightning discharge*, Academic Press, Orlando, 1987.

Uman, M.A., The earth and its atmosphere as a leaky spherical capacitor, *Am. J. Phys., 42*, 1033, 1974.

V. P. Pasko, U. S. Inan, and T. F. Bell, STAR Laboratory, Stanford University, Stanford, CA 94305.

Y. N. Taranenko, NIS-1, MS-D466, Los Alamos National Laboratory, Los Alamos, NM 87545.

(Received September 29, 1994;
revised November 7, 1994;
accepted December 13, 1994.)